Modeling Permanent Deformation of Flexible Pavements due to Overload with Finite Element Method

by

Seetharami Seelam, M.S. C.S.,
Roberto Osegueda, Ph.D., PE
Soheil Nazarian, Ph.D., PE

TECHNICAL REPORT STANDARD TITLE PAGE

1. Report No. TX-09 1502	2. Government Accession No.	3. Recipient's Catalog No.		
4. Title and Subtitle Model Calibrations with Local Accelerated Pavement Test Data and Implementation for Focused Solutions to NAFTA Problems		5. Report Date February 2003		
		6. Performing Organization Code		
7. Author(s) S. Seelam, R. Osegueda, and S. Nazarian		8. Performing Organization Report No. Research Report TX-1502-2		
9. Performing Organization Name and Address Center for Highway Materials Research The University of Texas at El Paso El Paso, Texas 79968-0516		10. Work Unit No.		
		11. Contract or Grant No. Study No. 5-1502		
12. Sponsoring Agency Name and Address Texas Department of Transportation P.O. Box 5051 Austin, Texas 78763		13. Type of Report and Period Covered Interim Report Sept. 1st, 2000 – May. 1st, 2003		
		14. Sponsoring Agency Code		

15. Supplementary Notes

Research Performed in Cooperation with TxDOT, LADOTD, NYDOT and FHWA under Project entitled "Model Calibrations with Local Accelerated Pavement Test Data and Implementation for Focused Solutions To NAFTA Problems"

16. Abstract

The objective of this study is to integrate the accelerated pavement test technologies of Texas, Louisiana and other participating States with modeling capabilities developed by the FHWA in their Truck Pavement Interaction (TPI) program. The pavement damage predictions have been made using a calibrated version of the VESYS 5 mechanistic/predictive model, which have been under development by the FHWA for the past two decades. During the course of this project, VESYS5 has been calibrated with the accelerated pavement test (APT) data from Texas. In this project, UTEP's role has been to develop a finite element model that can be used to predict permanent deformation of the pavement under NAFTA truckloads. These models, which have been primarily developed using finite element software package ABAQUS, provide tremendous flexibility that is not possible with VESYS5. For example, the three dimensional aspects of loading, as well as the impact of the load-induced nonlinear nature of material properties on the response of the pavement are rigorously modeled.

17. Key Words Pavement response, Rutting, VESYS5, Finite Element Analysis,		18. Distribution Statement No restrictions. This document is available to the public through the National Technical Information Service, 5285 Port Royal Road, Springfield, Virginia 22161		
19. Security Classif. (of this report) Unclassified	20. Security Classif. (of this page) Unclassified		21. No. of Pages 39	22. Price

The contents of this report reflect the view of the authors, who are responsible for the facts and the accuracy of the data presented herein. The contents do not necessarily reflect the official views or policies of the Texas Department of Transportation, Louisiana Department of Transportation and Development, New York State Department of Transportation or the Federal Highway Administration. This report does not constitute a standard, specification, or regulation.

The material contained in this report is experimental in nature and is published for informational purposes only. Any discrepancies with official views or policies of the Texas Department of Transportation, Louisiana Department of Transportation and Development, New York State Department of Transportation or the Federal Highway Administration should be discussed with the appropriate Austin Division prior to implementation of the procedures or results.

NOT INTENDED FOR CONSTRUCTION, BIDDING, OR PERMIT PURPOSES

Seetharami Seelam, M.S. C.S.
Roberto Osegueda, Ph.D., P.E. (82737)
Soheil Nazarian, Ph.D., P.E. (69263)

Acknowledgements

Abstract

The objective of this study is to integrate the accelerated pavement test technologies of Texas, Louisiana and other participating States with modeling capabilities developed by the FHWA in their Truck Pavement Interaction (TPI) program. The pavement damage predictions have been made using a calibrated version of the VESYS 5 mechanistic/predictive model, which have been under development by the FHWA for the past two decades. During the course of this project, VESYS5 has been calibrated with the accelerated pavement test (APT) data from Texas. In this project, UTEP's role has been to develop a finite element model that can be used to predict permanent deformation of the pavement under NAFTA truckloads. These models, which have been primarily developed using finite element software package ABAQUS, provide tremendous flexibility that is not possible with VESYS5. For example, the three dimensional aspects of loading, as well as the impact of the load-induced nonlinear nature of material properties on the response of the pavement are rigorously modeled.

Implementation Statement

This study is aimed at addressing the possible premature failure of flexible pavements caused by changes in size and weight requirements as the results of the NAFTA agreement. The outcomes of the finite element models developed here can readily be used to more accurately assess the magnitude of the damage that can be anticipated. However, the analysis is sometimes time consuming.

Currently, UTEP team is in the process of training artificial neural networks to accelerate the implementation of the finite element models.

TABLE OF CONTENTS

LIST OF FIGURES

LIST OF TABLES

CHAPTER ONE

INTRODUCTION

The implementation of the North American Free Trade Agreement (NAFTA) among Canada, Mexico, and the United States has re-focused the attention of some border highway agencies on the need to understand the impact of heavier axle loads and new axle configurations on their highway networks. Highways designed to carry vehicle loads of 80 kips (350 KN) could be trafficked with gross loads of over 120 kips (500 KN). New tire and axle configurations are also major concerns. Specialized haulage vehicles in Mexico are equipped with "super-single" tires. Tridem-axles and triple trailers are used on many long haul routes in Canada. The use of these heavy loads and different vehicle configurations will have a major impact on the performance of the US highway network. Hence, highway agencies urgently need defensible systems to predict the additional damage and the economic impacts of allowing such trucks in the US highway system.

This pooled fund study is aimed at providing these tools. The work-horse of this effort has been the VESYS 5 pavement damage prediction model calibrated with local materials and performance data. The latest version of VESYS includes the capability to include both tandem and tridem-axles and prediction of the rutting within each pavement layer. This is based upon the computed strains in each layer together with the layer material parameters of μ and α. The parameter μ represents the proportionality between the permanent and elastic strains, and α indicates the rate of increase in permanent deformation against the number of load applications. Both of these parameters can be obtained from the laboratory or backcalculated from accelerated pavement testing (APT) data.

To address the issue of defensibility of damage prediction, controlled pavement performance data generated in accelerated pavement testing programs around the US can be used. For example, in the Texas Mobile Load Simulator (TxMLS) program, the increase in layer deformations under load has been monitored using sophisticated pavement instrumentation. This data has been used extensively in this study to calibrate the models prior to making predictions with either overloads or new axle configurations.

Despite the successes in VESYS 5 for the rutting and performance predictions in pavement systems, some limitations exist. For example, new or more advanced constitutive models cannot be easily

included into VESYS 5. Also scenarios, such as the impact of moving loads, temperature and three-dimensional state of stress, cannot be considered. Finite Element (FE) techniques, on the other hand, generally possess flexibility in the adoption of emerging constitutive models. And, with the advances of computer CPU power, the codes are usually readily available on engineers' personal computers.

Chapter 2 of this report contains a brief review of the literature. In chapter 3, the methodology followed to select a packaged Finite Element program is described. Chapter 4 contains a description of the models implemented in the finite element program to determine the permanent deformation of pavements. The calibration and validation of the models are included in Chapter 5. Chapter 6 is dedicated to the three-dimensional models developed for this project. Chapter 7, the last chapter, includes the summary of the work accomplished, the work remaining and the status of the project.

CHAPTER TWO

BACKGROUND

A large number of papers and reports document the use of finite element analyses for modeling rutting and permanent deformations. Saliba (1990) presented a brief review of the mathematical theory of visco-plasticity and the computational procedure used in a finite-element program to model tire/soil interaction.

Zaghloul and White (1994) developed a procedure for permitting overloaded trucks in Indiana. Load Equivalency Factors (LEF) for asphalt pavements with granular base as well as for full depth asphalt pavements were developed. As a part of this study a three-dimensional, dynamic finite element program (3D-DFEM) was used to develop load equivalency factors. Truck loads moving at different speeds were included in the analysis and a number of material models were used to represent the actual pavement materials behavior under moving loads.

Rowe et al. (1995) developed a method of analysis based on improved material characteristics to accurately reflect fatigue cracking and permanent deformation performance. Their work focused on the dissipated energy fatigue criterion, a visco-elastic materials characterization, and a pavement analysis using the finite-element method for determining the response to repeated wheel loading.

Kirkner et al. (1996) addressed complexities associated with the modeling of pavement systems using the finite element method, in particular those associated with moving loads, non-linear material behavior and the unbounded domain. They discussed a methodology that is based on a steady-state assumption and the use of a moving coordinate system.

Ramsamooj et al. (1998) presented an elasto-plastic model for predicting the stress/strain response of asphalt concrete under cyclic loading. They used multi-yield surfaces and isotropic hardening, Rowe's stress dilatancy theory to obtain the relationship between the permanent volumetric and vertical strains, and a hardening law for the changes in the sizes of the plastic moduli caused by cyclic loading.

Chen and Tsai (1999) evaluated the effects of linear viscoelastic properties of asphalt on pavement rutting and fatigue cracking. They calculated the dissipated energy per traffic cycle to directly relate the linear viscoelastic properties of asphalt binders to the pavement performance.

Seibi et al. (2001) modeled the tendency of AC to behave elastically and visco-plastically during cold and hot seasons, respectively. The visco-plastic response was characterized by the rate dependency of the plastic response and was found to be linearly strain hardening. The model used a yield criterion based on the loading function defined by Drucker-Prager. They calibrated their models through an optimization process that involved iterative calls between finite element results and the optimum parameters to develop a generalized elastic-visco-plastic constitutive relation for AC.

Blab and Harvey (2002) used a 3-dimensional FE model of a road pavement in which the temperature and load dependent performance of flexible pavements was characterized by a generalized Maxwell model. The model was evaluated using simulation calculations for a specific test structure on which rutting tests had been performed with a heavy vehicle simulator. This evaluation demonstrated good agreement between the deformations predicted by the theoretical model and the deformations actually measured.

Hossain and Wu (2002) used a three-dimensional (3-D) non-linear finite element model to simulate the initiation and propagation of rutting damage on the Superpave test sections of the Kansas Accelerated Testing Laboratory. A creep and Drucker-Prager model was chosen to characterize the permanent deformation characteristics of the Superpave mixtures and the aggregate base and subgrade materials, respectively.

Werkmeister et al. (2002) discuss the use of shakedown approach to characterize the deformation behavior of unbound granular materials (UGM) in pavement construction. The essence of a shakedown analysis is to determine the critical shakedown load for a given pavement. The Dresden material law was introduced for modeling the permanent and resilient deformation behavior of UGM layers in pavement constructions under consideration of the shakedown ranges. They also described a design method that uses test results from the repeated load triaxial tests to establish the risk level of permanent deformations in the UGM layers using a nonlinear resilient material law implemented into a FE Program called FENLAP.

Long et al. (2002) discussed the development of a constitutive model that describes the permanent deformation behavior of asphalt concrete. The model was implemented in a finite element code, and simulation of laboratory and heavy vehicle simulator tests are used to validate the model.

The authors cited share in common that some degree of success was accomplished with the FE method in correlating the predicted rutting and permanent to experimental field or laboratory data. Our goal is to take advantage of many years of experience with VESYS to develop FE models that can be readily used to predict the behavior of pavements under more realistic boundary conditions.

CHAPTER THREE

EVALUATION OF FINITE ELEMENT PROGRAMS

The first step in this research work was to select an existing finite element software package that can conveniently achieve the goals of the project. ALGOR and ABAQUS, commonly used by researchers and practitioners in the engineering field, were considered for evaluation. The criteria used for the evaluation of the software are as follows:

- accuracy of the results,
- cost of purchasing or licensing the software for commercial use by the participating highway agencies,
- ease of inputting data into the software and retrieving output from the software, and
- ease of implementing material constitutive models that are appropriate to this study.

The results from the evaluation of the two finite element programs based on the above criteria are presented below. ABAQUS was eventually proposed for this study.

ACCURACY OF RESULTS

The first and foremost important criterion in choosing a particular program is its ability to provide accurate solutions to real-world problems. No matter how flexible and how efficient, there is no point in using a software that does not provide accurate results. A way to judge the accuracy of a finite element software is to build and analyze a model in that package for quantities such as deflection, stresses, etc.

A pavement structure was modeled using a 2-D axi-symmetric finite element model, in the two software packages. The pavement structure consists of 3 layers as shown in Figure 3.1. The material properties used in those models are shown in Table 3.1. The models were subjected to a circular loading 5 in. (125 mm) radius and an intensity of 100 psi (69 kPa). The parameter used to judge the accuracy of the software packages was the vertical surface deflection on top of the AC
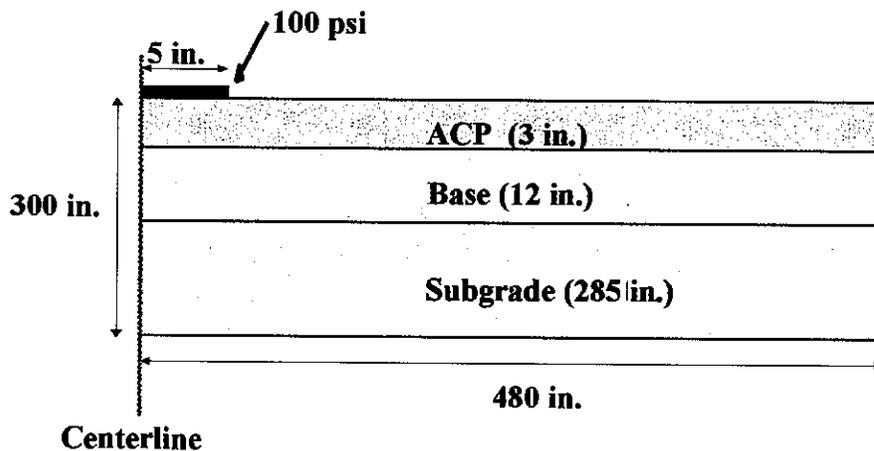
Figure 3.1 - Typical Pavement Section used for Determining Accuracy of Finite

Table 3.1 - Material Properties of the above typical pavement section used in Validating Finite Element Models

Layer Name	Modulus (psi)	Poisons Ratio
ACP	500000	0.35
Base	50000	0.3
Subgrade	10000	0.40

layer. Surface deflections at seven locations were extracted from the two programs at 12 in. intervals from the centerline of the model (i.e., at 0 in., 12 in., 24 in., ... 72 in.). The extracted deflections are plotted in Figure 3.2 along with the deflections obtained by the linear elastic layered model BISAR. The deflections in all three cases are within 1% of each other. Hence, in terms of accuracy, both packages (ALGOR and ABAQUS) are satisfactory

PRICE OF LICENSING SOFTWARE

The second criterion was the cost of purchasing or licensing the software for commercial use by the participating highway agencies. At the time of preparation of this document the cost for acquiring either of the software's is comparable. As such, the cost of licensing any of the two software packages is equally favorable.

EASE OF USE

The third criterion was the ease of inputting data into and retrieving output from the software. The software should be easy to learn, easy to modify the input information, and easy to retrieve the

6

Figure 3.2 - Variations in Deflections from ALGOR, ABAQUS and BISAR for Model shown in Figure 3.1

output information at the end of the analysis. As a part of our research, optimized meshes ("standard" mesh) have been developed so that the practitioners in the field can modify them according to their requirements. For example, a "standard" model 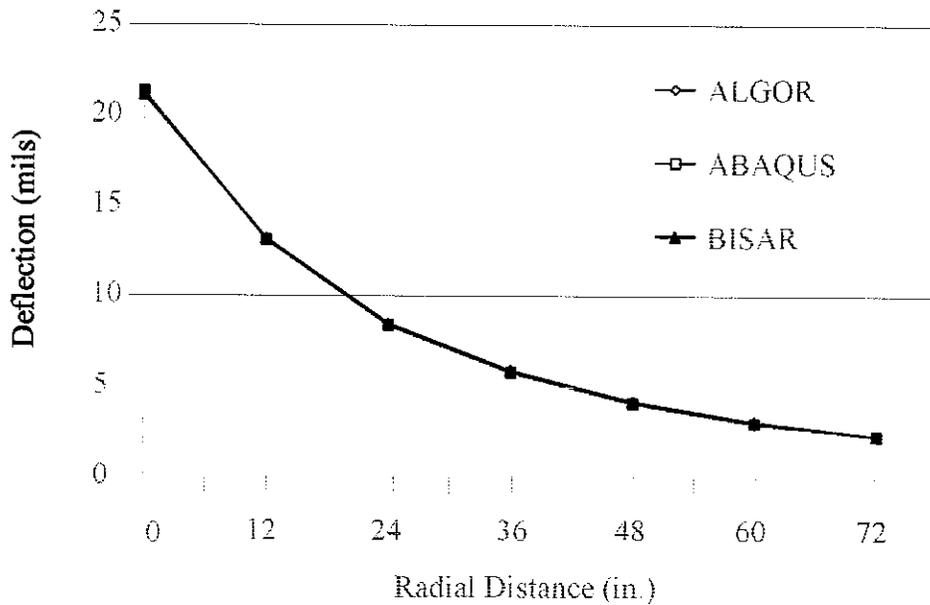can be used to determine the effects of change in thickness of a particular layer on the life of the pavement. The "standard" models can even be used to build an entirely new model with new material properties, creep parameters, load configurations, load positions, geometric properties, etc. The two finite element programs are evaluated on this basis.

ALGOR provides an easy-to-use user interface to build finite element meshes, input load configurations, input material properties, etc. The results of the analysis can be conveniently inspected through a visualization module. However, to increase or decrease the layer thickness, width or length of the pavement, or to alter load configuration, a new mesh has to be built from scratch, which is time consuming and laborious.

ABAQUS also has an easy to use user interface to build finite element meshes, and to input load configurations and material properties. A visualization module to inspect the results of the analysis is also available. Contrary to ALGOR, an input file generated by ABAQUS can be modified to cater to different needs. The modifications include increase or decrease in layer thickness, change in the width of the pavement, or alter load configuration, etc. As such, a new analysis can be carried out without creating a new finite element model. This feature provides a more convenient and faster mesh building process as compared to ALGOR. In this viewpoint, ABAQUS has an advantage over ALGOR for this research.

EASE OF IMPLEMENTATION OF NEW MATERIAL MODELS

The fourth and the last criterion in choosing a finite element program was the ease of implementing new material constitutive models in the finite element software package that are appropriate for this study.

In order to determine the permanent deformation under NAFTA truckloads, the selected finite element software package must be able to perform rutting analysis. For rutting analysis of a multilayer system, the permanent deformation of each layer is modeled using a general power-law creep constitutive model in the form of

$$\varepsilon_{(p)}(t) = C_1 \cdot (\sigma)^{c_2} \cdot t^{c_3} \tag{3.1}$$

where $\varepsilon_{(p)}(t)$ = the permanent strain after time t, σ = is the axial stress with C_1 through C_3 being equation constants.

The permanent deformation in a multilayer system accumulates as time progresses. The rate of accumulation of permanent deformation is initially rapid but gradually decreases. In order to obtain such a trend, the constant C_3 must always be negative (i.e. $C_3 < 0$). The power law creep model implemented in ALGOR is a strain-hardening model. As such, the time exponent C_3 can only vary between 0 and 1. This restriction prohibited us from using ALGOR for this research.

In ABAQUS, the power law creep model is implemented using both strain-hardening form and in the corresponding time-hardening form. The time hardening form of the power law model is:

$$\overline{\varepsilon}^{cr} = A \cdot \tilde{q}^n \cdot t^m \tag{3.2}$$

where $\overline{\varepsilon}^{cr}$ is the uniaxial equivalent creep strain rate, $\tilde{q}$ is the uniaxial deviatoric stress, t is the total time and A, n and m are equation constants.

The biggest advantage of ABAQUS power law creep model is that the exponent of time, m, can take any value between -1 and 0. Hence, the ABAQUS power law creep model can be used to predict permanent deformation in pavements. Another advantage of using ABAQUS is that the time hardening form of power law model can be modified as per user requirements using user-defined subroutines. This feature of ABAQUS offers great flexibility over other finite element software packages.

From the above analysis, ABAQUS has the following advantages over ALGOR:

- It is easy to alter the standard input data file generated in ABAQUS to generate finite element meshes for different layer thickness; whereas a new model has to be built from scratch with ALGOR for every analysis with varying geometric properties.

8

- The power law creep model built in ALGOR cannot be used for the analysis of permanent deformation of pavements, while the power law creep model built in ABAQUS can be used for that purpose.
- Users can define their own material models using ABAQS though user-defined subroutine. This is not possible in ALGOR.

In summary, both software packages are in general user-friendly and easy-to-use. For our project, ABAQUS was the more feasible option.

CHAPTER FOUR

MODELING PERMANENT DEFORMATIONS

To estimate the progression of rutting with load repetition using layer elastic theory (e.g. as carried out in VESYS) all layers are modeled using a constitutive model in the form of

$$\frac{d\varepsilon_{(p)}}{dN} = \mu \cdot \varepsilon_r \cdot N^{-\alpha} \qquad (4.1)$$

where $\varepsilon_p(N)$ = permanent strain, ε_r = resilient elastic strain, N = load cycle number and μ and α are material parameters often measured in the laboratory. From Equation 4.1, permanent deformation after any numbers of load cycles is obtained through the following integration:

$$\Delta\varepsilon_{(p)} = \varepsilon_{pN2} - \varepsilon_{pN1} = \frac{\mu}{1-\alpha} \cdot \varepsilon_r \cdot \left[N^{-\alpha-1} \right]_{N1}^{N2} \qquad (4.2)$$

The accumulated permanent strain can be determined from:

$$\varepsilon_{(p)} = \frac{\mu}{1-\alpha} \cdot \varepsilon_r \cdot N^{-\alpha-1} \qquad (4.3)$$

Usually, layer elastic models such as VESYS obtain ε_r after the 200th cycles of load are applied. Practically speaking, this assumption could lead to some approximations because the resilient strain changes after every load cycle. In FE models, the resilient strain can be determined after each load cycle and used to calculate the accumulated strains in Equation 4.3.

MODELING PERMANENT DEFORMATIONS USING ABAQUS

To accommodate the power law creep model described by Equation 4.1 in ABAQUS, a standard power-law creep model in the following form was used

$$\frac{d\varepsilon_{cr}(t)}{dt} = A\widetilde{q}^n t^m \tag{4.4}$$

where $\varepsilon_{cr}(t)$ is the permanent creep strain per unit time, $\widetilde{q}$ is the equivalent von Misses stress, t is the total time and A, n and m are constants associated with material parameters. The creep strain is obtained by integration similar to the one performed for the layer elastic creep model in the following form:

$$\Delta\varepsilon_{cr} = \varepsilon_{cr_1} - \varepsilon_{cr_2} = \frac{A}{1+m}\widetilde{q}^n \left[t^{1+m} \right]_{t_1}^{t_2} \tag{4.5}$$

where:

$$\widetilde{q} = \sigma_e = \sqrt{\frac{1}{2}\left\{ (\sigma_1 - \sigma_2)^2 + (\sigma_2 - \sigma_3)^2 + (\sigma_3 - \sigma_1)^2 \right\}} \tag{4.6}$$

with σ_i's ($1 \leq i \leq 3$) being the principal stresses.

One should note that the Von Misses stress $\widetilde{q}$ has an associated strain. This uniaxial elastic strain, $\widetilde{\varepsilon}_e$, can be calculated from:

$$\widetilde{\varepsilon}_e = \frac{\sqrt{2}}{3}\sqrt{(\varepsilon_1 - \varepsilon_2)^2 + (\varepsilon_2 - \varepsilon_3)^2 + (\varepsilon_3 - \varepsilon_1)^2} \tag{4.7}$$

where ε_i's ($1 \leq i \leq 3$) are the principal strains. To accommodate the layer elastic creep model in ABAQUS, the standard power law creep model is modified using ABAQUS user defined subroutine CREEP assuming that the equivalent elastic uniaxial strain is the resilient strain. The resulting equation is:

$$\frac{d\varepsilon_p}{dN} = \mu\widetilde{\varepsilon}_e N^{-\alpha} \tag{4.8}$$

To convert time, t, to the number of cycles, N, one can simply assume that one cycle of load would last one unit of time. The integration of the above equation is performed similar to the one shown for layer elastic model, but the integration in finite elements is performed for all elements in the model, not only for the elements in the vicinity of the load as in layer elastic model.

12

The above model as implemented in ABAQUS was used with the material parameters measured at a site to obtain the variation in rutting with load. As an example, the results from one site are included here. The site, which was trafficked by the TxMLS device, is located on US281 near Jacksboro, TX. Typical cross-section of the site consisted of 8 in. (203 mm) of AC layer over 15 in. (381 mm) of base over a subgrade. The stiffness of the layers with time was regularly measured at this site. The variation in modulus of the AC with time can be simplified into five seasons. The typical temperature, ACP moduli, and α and μ parameters for each season are given in Table 4.1. A Poisson's ratio of about 0.33 was assumed for that layer. The relevant material parameters for the base and subgrade layers are summarized in Table 4.2. The same material parameters were used for the base and subgrade layers. It should be mentioned that the material parameters in Tables 4.1 and 4.2 were provided to us by our collaborators at the Texas Transportation Institute (see Zhou and Scullion 2002).

Table 4.1 – Material Parameters for Asphalt Concrete Layer of US281 Northbound (from Zhou and Scullion , 2002)

Season	Temp. (°F)	Parameter α	Parameter μ	Modulus (ksi)
1	89	0.610	0.260	211
2	84	0.638	0.263	243
3	92	0.598	0.250	194
4	95	0.568	0.245	180
5	91	0.598	0.259	200

Table 4.2 – Material Parameters for Base and Subgrade Layers of US281 Northbound (from Zhou and Scullion , 2002)

Layer	Parameter	Value
Base	Modulus	38 ksi
	Poisson's Ratio	0.38
	Parameter α	0.10
	Parameter μ	0.78
Subgrade	Modulus	8 ksi
	Poisson's Ratio	0.40
	Parameter α	0.01
	Parameter μ	0.75

The variation in rut depth with the number of load repetition for the representative temperatures included in Table 4.1 is shown in Figure 4.1. As anticipated, the rut depth is greater at higher temperatures.
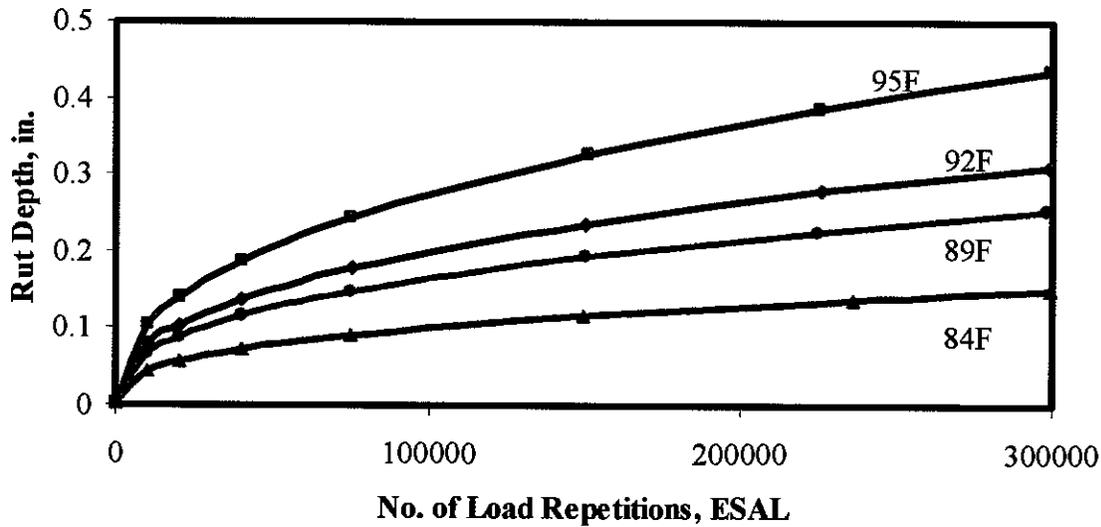
Figure 4.1 - Variation in Rut Depth with Load Repetition at Different Temperature from ABAQUS

curves are obtained. Let us assume that K_i ($1 \leq i \leq N$) corresponds to the number EASLs for each season. The total number of load cycles T is then given by:

$$T = \sum_{i=0}^{N} K_i \qquad (4.9)$$

The actual rut depth as a function of ESALs from the N rut depth-ESAL curves (the solid curve in Figure 4.2) can be obtained by combining them in the following manner. For the first K_1 ESALs, corresponding to the first season, the rut depth-ESAL curve corresponding to the first season (shown in Figure 4.2 as a dashed curve) is used. In the figure, the ESALs are converted to actual time by simply dividing the number of load applications by the projected number of ESALs. For any other season, the curve corresponding to that season is shifted horizontally until the rut depth from the general curve and the one under consideration coincide. This process is repeated for all seasons as shown in Figure 4.3. The data points are then combined to obtain the overall rut depth vs. traffic (or time) as shown with solid line in Figure 4.3.

NONLINEAR α AND μ PARAMETERS

In the previous section, it was assumed that α and μ are linear. Recent study by Zhou and Scullion (2002) demonstrated that α and μ are stress and temperature dependent, and as such are nonlinear. These nonlinear models for α and μ can be readily incorporated in the FE model.
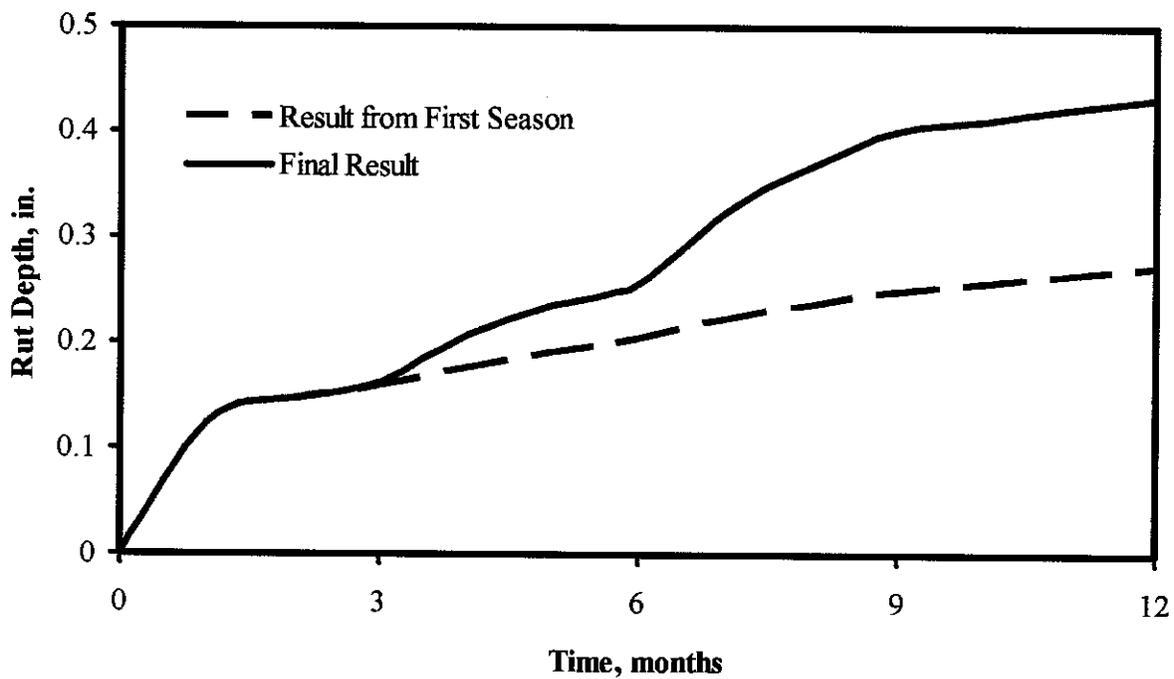
14

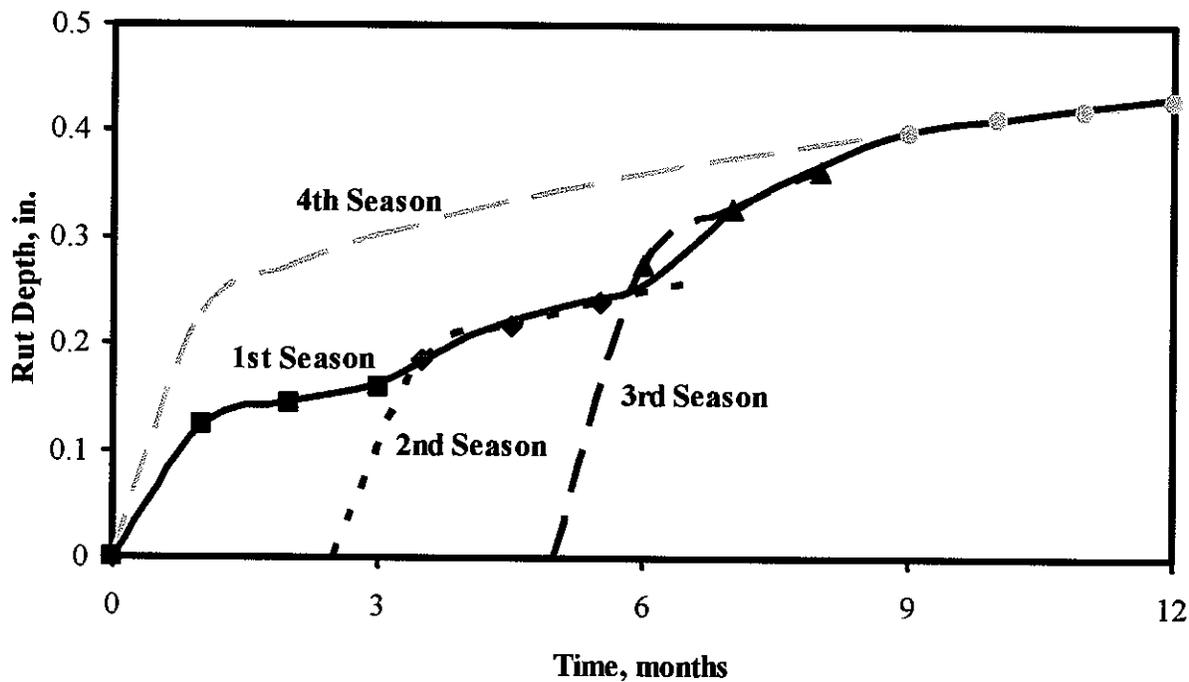**Figure 4.2 – Initial Step in Reconstructing Rut depth curve**

Figure 4.3 – Constructing Final Rut Depth vs. Time Curve

Zhou and Scullion conducted a series of lab tests on 4 in. (100 mm) diameter by 6 in. (150 mm) height cylindrical specimens as shown in Figure 4.4. They subjected the specimens to different confining pressures (σ_3) and axial stresses (σ_1) and different temperatures to measure the permanent deformation with the number of load cycles. Typical accumulated permanent strain with the number of loads applied is also shown in Figure 4.4. Such a curve can be used to backcalulate the α and μ parameters for a given stress and temperature regimes.

Zhou and Scullion propose the following equations to determine the α and μ:

$$\alpha = 1.748418 - 0.446558 \log T - 2.65284 \frac{\log \sigma_D}{34.03532 - 0.253679T} \qquad (4.10)$$

$$\mu = 1.663759 - 0.438729 \log T - 1.25191 \frac{\log \sigma_D}{1.918523 + 0.066875T} \qquad (4.11)$$

where, T is the temperature of the pavement expressed in $^\circ$F, and $\sigma_D = \sigma_1 - \sigma_3$ is the deviator stress expressed in psi.

To test the validity of the nonlinear parameters α and μ, the test process described above was simulated in the ABAQUS. The finite element mesh shown in Figure 4.5 incorporated with the nonlinear α and μ, parameters as described in Equations 4.10 and 4.11 were executed for various deviatoric stresses and temperatures. Typical deformation within a specimen tested at a temperature of 122 $^\circ$F (50 $^\circ$C) and a confining pressure of 20 psi (140 KPa) is shown in Figure 4.5. The lab and FE results compare favorably up to a deviatoric stress of 100 psi (690 KPa). The results from the 120 psi tests do not seem to be close. The reason for this anomaly, aside from the experimental errors, is unknown at this time. The nonlinear parameters shown here can be readily implemented in the finite element models.
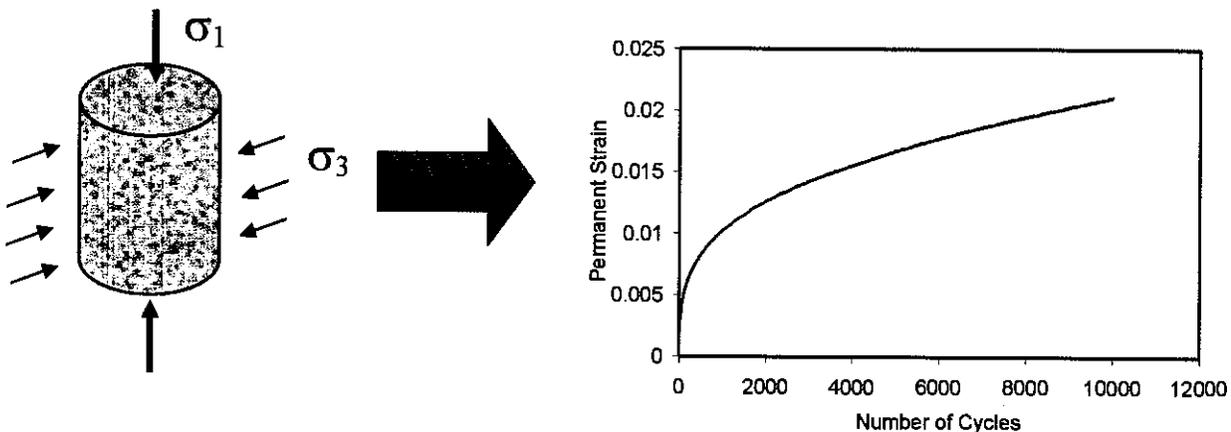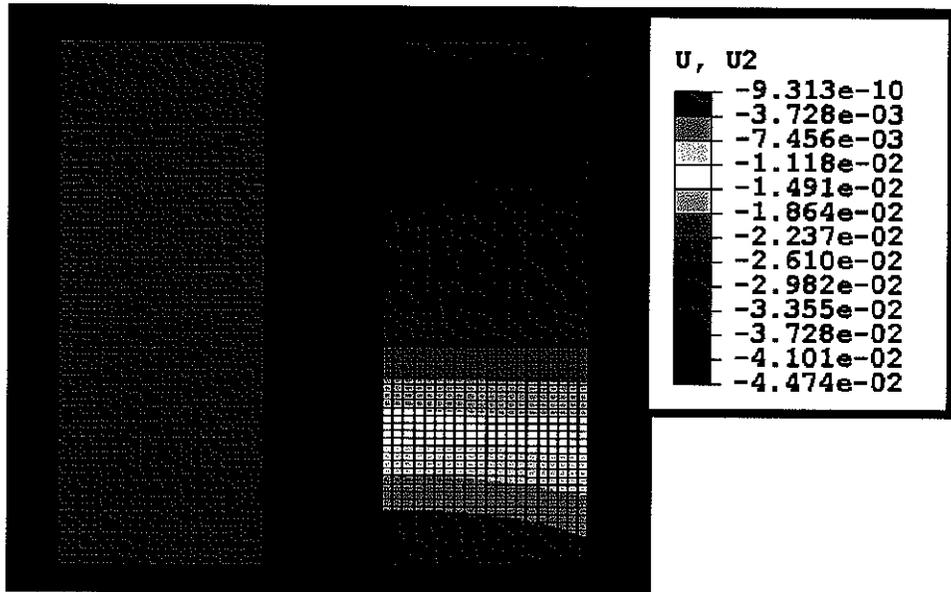

Figure 4.4 –Laboratory Tests to Obtain Parameters α and μ

U, U2
 -9.313e-10
 -3.728e-03
 -7.456e-03
 -1.118e-02
 -1.491e-02
 -1.864e-02
 -2.237e-02
 -2.610e-02
 -2.982e-02
 -3.355e-02
 -3.728e-02
 -4.101e-02
 -4.474e-02

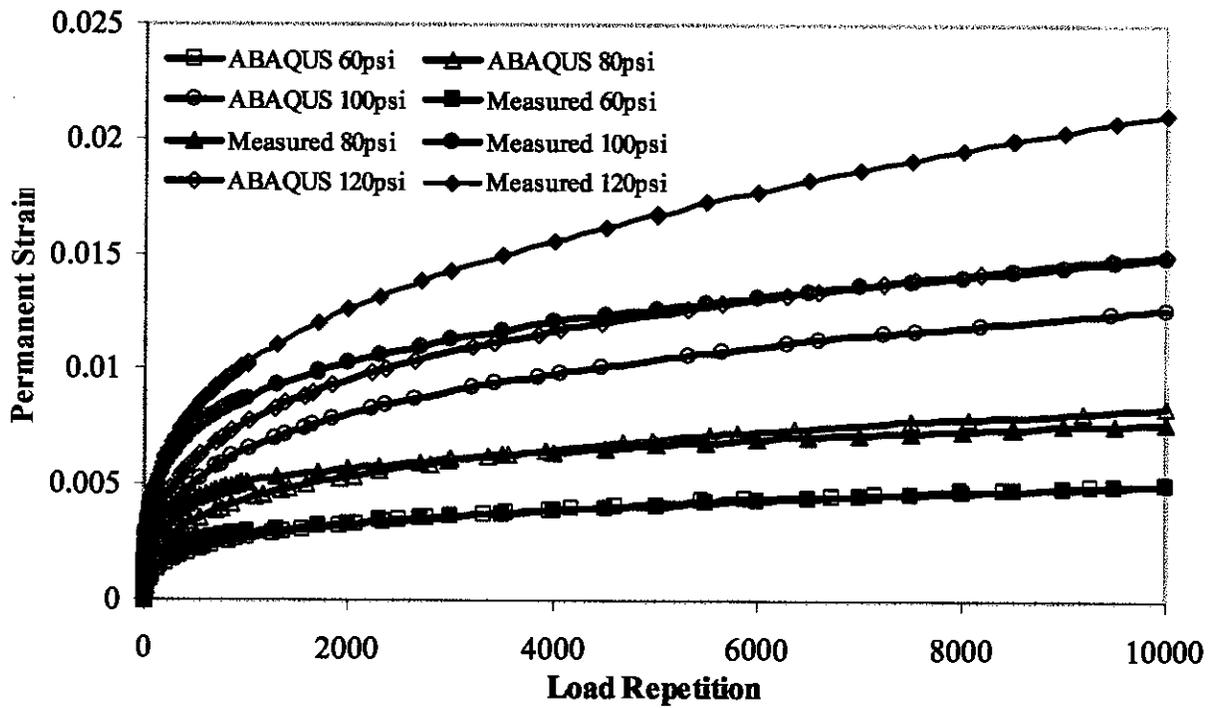**Figure 4.5 - Finite Element Simulations of Lab Tests**

Figure 4.6 - Comparison of Lab and Simulated Results

18

CHAPTER FIVE

CALIBRATION OF ABAQUS FINITE ELEMENT MODEL AND OVERLOAD ANALYSIS

A dense and highly refined mesh, especially in the vicinity of the applied loads, is necessary to obtain accurate results from any finite element analysis. Such refinement is not necessary at places where the stress gradient is not large. If the mesh is too refined, the computational time will be excessive. The goal of the optimization process is to determine the minimum number of elements needed to obtain representative results.

Finite element meshes can be constructed in two ways with ABAQUS, either by using the ABAQUS/CAE software (a built-in pre- and post- processor module) or manually using a text editor. ABAQUS/CAE can be used for both mesh generation and visualization of the results. To demonstrate the advantages of the CAE over manual process, two meshes were optimized, one manually and another with the CAE. The pavement section used is the US 281 southbound MLS site described later in this chapter.

The two meshes after optimization are shown in Figures 5.1 and 5.2. The automatic mesh with the CAE has about 2,000 elements whereas the manual mesh has about 4,000 elements. As such, the computation time for the manual mesh is about twice as the computation time required executing the automatic one. The elastic deformations obtained with these two meshes under the same load conditions are compared with the elastic deformations obtained with the layer elastic program BISAR in Figure 5.3 at various temperatures. The impact of the change in temperature is a change in the modulus of the AC layer. The results from the three calculations are within 1% of one another.

In summary, the finite element meshes generated using the ABAQUS/CAE have the following advantages over those generated manually:

- meshing in regions with high stress gradients can be easily be refined,
- node compatibility at layer interfaces can easily be maintained, and
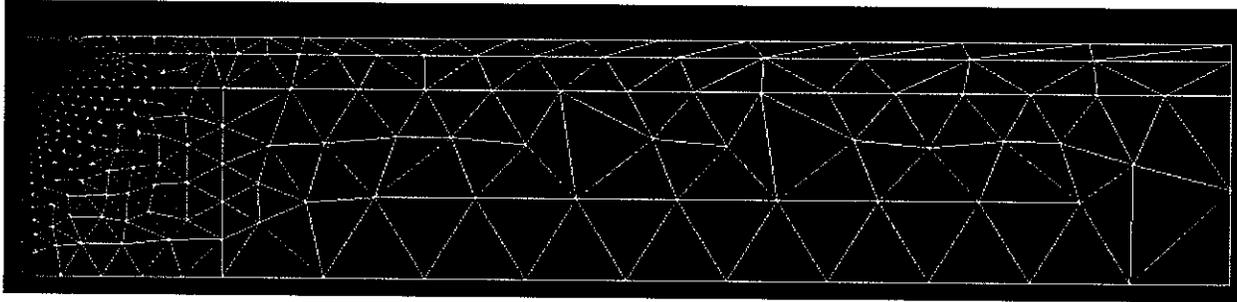- aspect ratio of elements can be maintained easily.

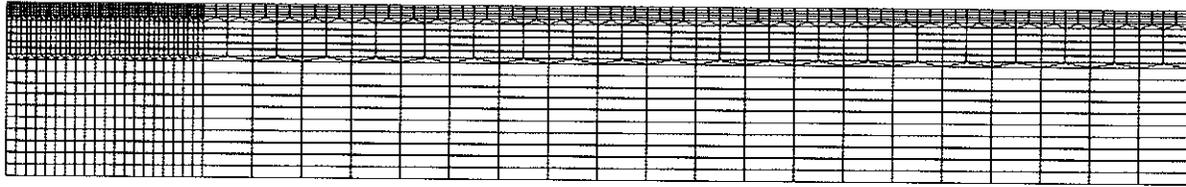**Figure 5.1 - Finite Element Mesh Generated with ABAQUS/CAE**

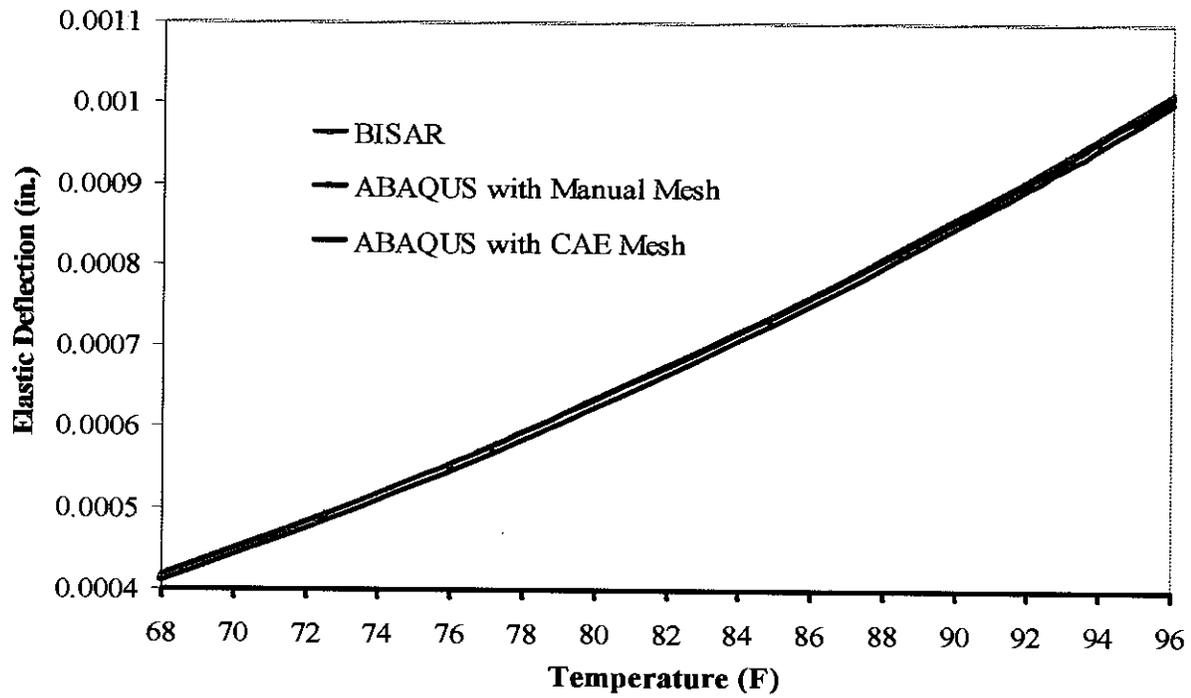**Figure 5.2 - Finite Element Mesh Generated Manually**

Figure 5.3 - Comparison of Elastic Deformations FROM ABAQUS AND BISAR

The material parameters used for the above comparison were provided by Zhou and Scullion (2002) for a site located on US281 Southbound in Jacksboro, TX. Typical cross-section of the site consisted of 7.25 in. (184 mm) of AC layer over 15 in. (381 mm) of base over a subgrade. The stiffness of the layers with time was regularly measured at this site. The variation in modulus of the AC with time can be simplified into ten seasons. The typical temperature, ACP moduli, and α and μ parameters for each season are given in Table 5.1. A Poisson's ratio of 0.33 was assumed for that layer. The relevant material parameters for the base and subgrade layers are summarized in Table 5.2. As indicated by Zhou and Scullion (2002), the material parameters in Tables 5.1 and 5.2 were backcalculated to match the rutting trends from the VESYS and field observations.

Table 5.1 – Material Parameters for Asphalt Concrete Layer of US281 Southbound (from Zhou and Scullion, 2002)

Season	Temp. (°F)	Parameter α	Parameter μ	Modulus (ksi)
1	72.5	0.701	0.260	696
2	68.0	0.712	0.280	814
3	84.9	0.670	0.240	473
4	95.0	0.608	0.210	359
5	91.0	0.628	0.225	399
6	94.0	0.612	0.212	369
7	96.0	0.602	0.208	350
8	93.0	0.616	0.217	379
9	77.2	0.690	0.250	597
10	76.0	0.694	0.252	620

Table 5.2 – Material Parameters for Base and Subgrade Layers of US281 Southbound (from Zhou and Scullion, 2002)

Layer	Parameter	Value
Base	Modulus	38 ksi
	Poisson's Ratio	0.38
	Parameter α	0.080
	Parameter μ	0.78
Subgrade	Modulus	8 ksi
	Poisson's Ratio	0.40
	Parameter α	0.005
	Parameter μ	0.76

The seasonal variations are incorporated into ABAQUS Finite Element Model and the rutting patterns calculated from different temperatures were combined using the algorithm described in Chapter 4, which is similar to VESYS. The results for both US 281 north bound and US 281 south bound were reasonably close as shown in Figures 5.4 and Figure 5.5.
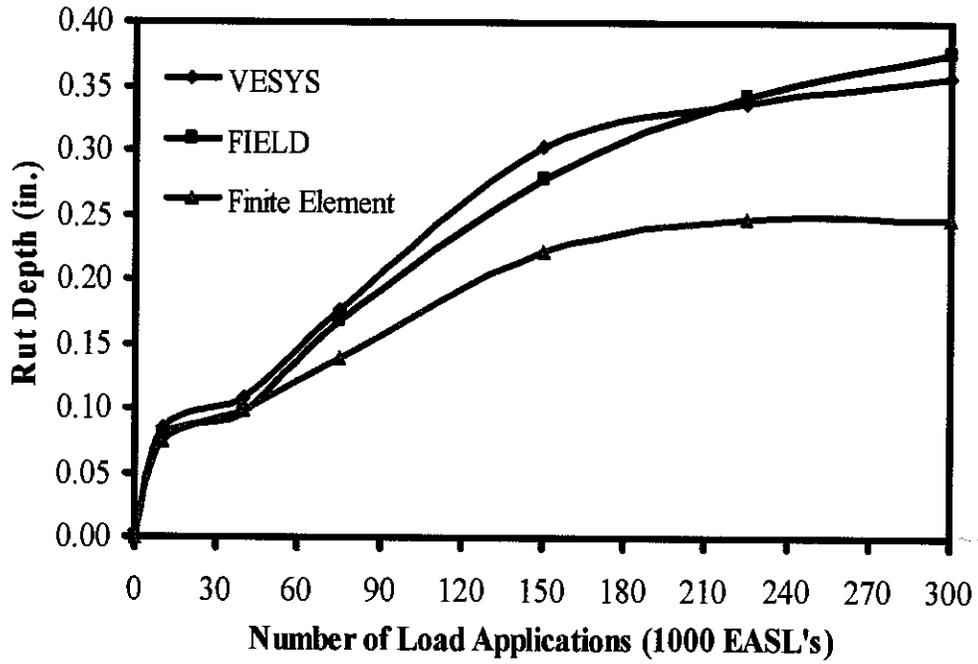
Figure 5.4 - Comparison of Rutting Trends from VESYS, ABAQUS with Trend Observed in the Field (US 281 North Bound)
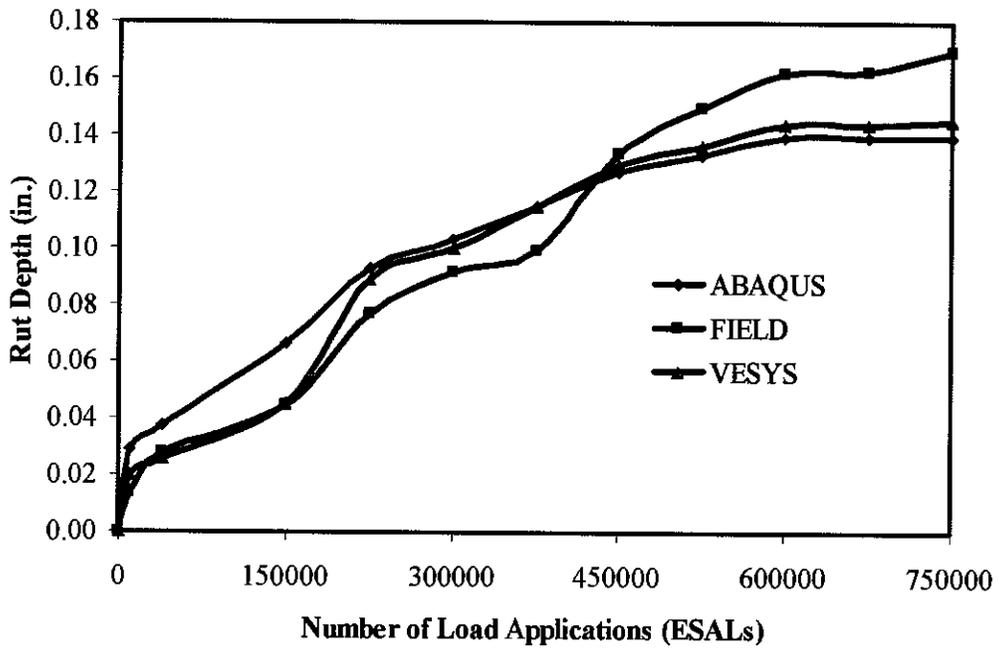

Figure 5.5 - Comparison of Rutting Trends from VESYS, ABAQUS with Trend Observed in the Field (US 281 Southbound)

RUTTING ANALYSIS OF OVERLOAD CASES

As described before, one of the objectives of the project was to study the impact of overload trucks. To study the impact of the overload on rutting, the nonlinear models presented in Equations 4.10 and 4.11 were implemented into the calibrated models from the north bound and south bound of the US 281 sites. In this study, load applied over the pavement is increased by 5% to 30% over the standard tandem load (34 kip). Rutting as a function of load repetitions for these conditions are shown in Figures 5.6 and 5.7. Increase in the amount of rutting is significantly greater than the increase in the applied load. Unfortunately, the overload field data was not available to verify the results. However, this example demonstrates that the nonlinear models can be readily used.
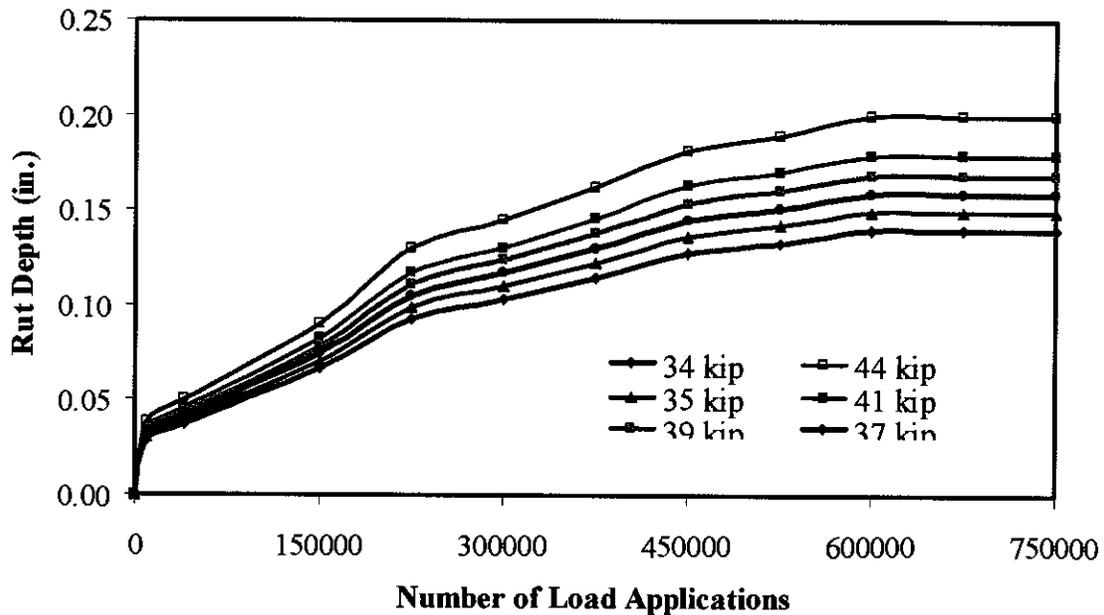
Figure 5.6 – Variations in Rutting with Number of ESALs for Different Applied Loads (US 281 Southbound)
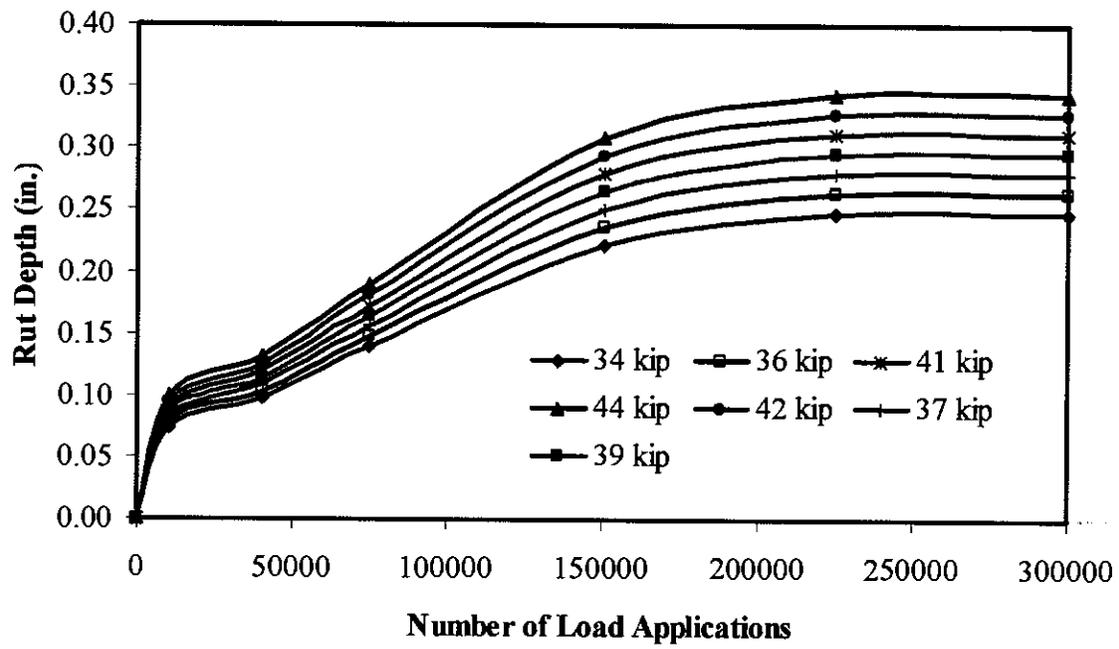
Figure 5.7 – Variations in Rutting with Number of ESALs for Different Applied Loads (US 281 Northbound)

CHAPTER SIX

THREE-DIMENSIONAL FINITE ELEMENT MODELING

INTRODUCTION

Two-dimensional axisymmetric models are traditionally used to estimate the rut depth under equivalent single axial loads (EASLs). The primary goal of this project is to evaluate the impact of over-weight vehicles as well as axle configurations that in many occasions may deviate form the equivalent single axle load configurations. To estimate the rut depth under more realistic conditions and pavement geometry, 3-D models are necessary. Three-dimensional models offer several advantages over axisymmetric ones. Actual load configurations can be readily modeled. Realistic geometric conditions such as edges, discontinuities and boundary conditions can be incorporated. These advantages, however, come at the expense of computation time and resources.

ABAQUS offers a wide variety of 3-D finite element shapes including pentahedral, hexahedral, and tetrahedral. Element type C3D8R (8-node linear brick element) is mostly used in this study. A 3-D mesh corresponding to the 2-D mesh shown in Figure 5.2 is shown in Figure 6.1. This model contains about 12,000 elements. A mesh with almost 40,000 elements was also developed for comparison purposes. The elastic deformations under the load at different temperatures from the 2-D model are compared with those from the two 3-D models in Figure 6.2. The deformations from the two 3-D meshes are virtually the same indicating that decreasing the number of elements down to 12,000 does not compromise the accuracy of the results. However, smaller number of elements provided results that deviated from the expected results. Also, the 2-D and 3-D results are fairly close demonstrating the integrity of the mesh developed. One less than obvious conclusion of this case study is that in order to obtain reasonable results, a large number of elements are needed. The computation time associated with such a mesh is prohibitive.
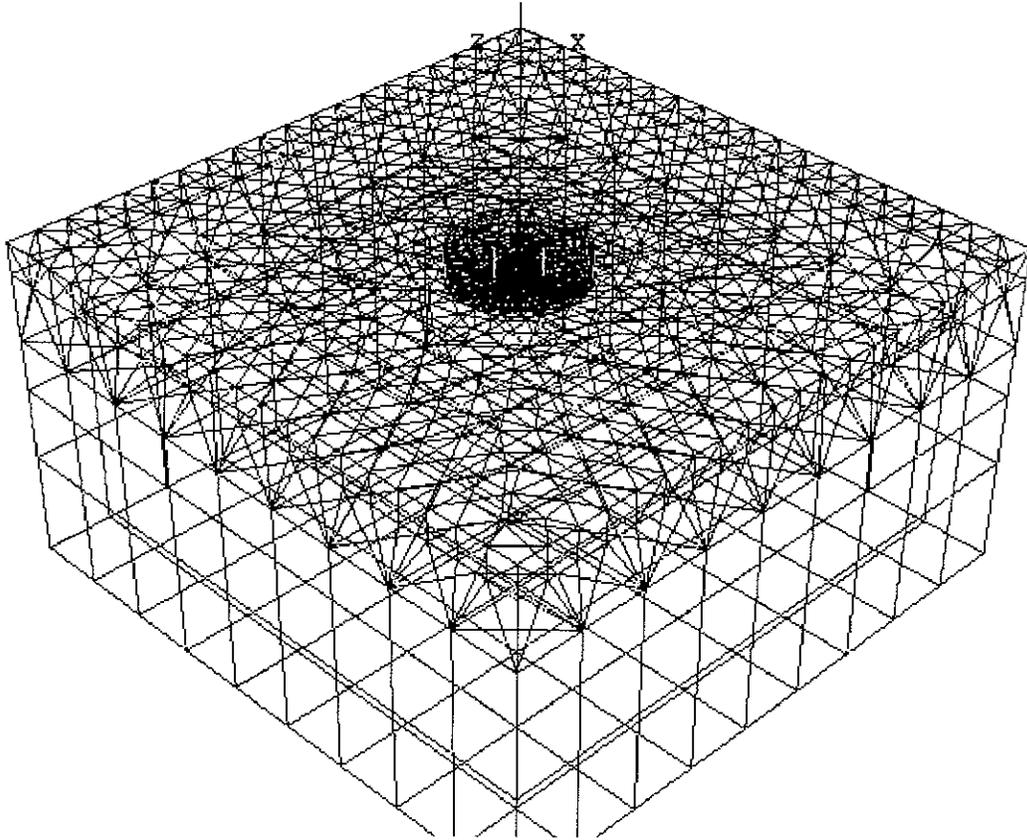
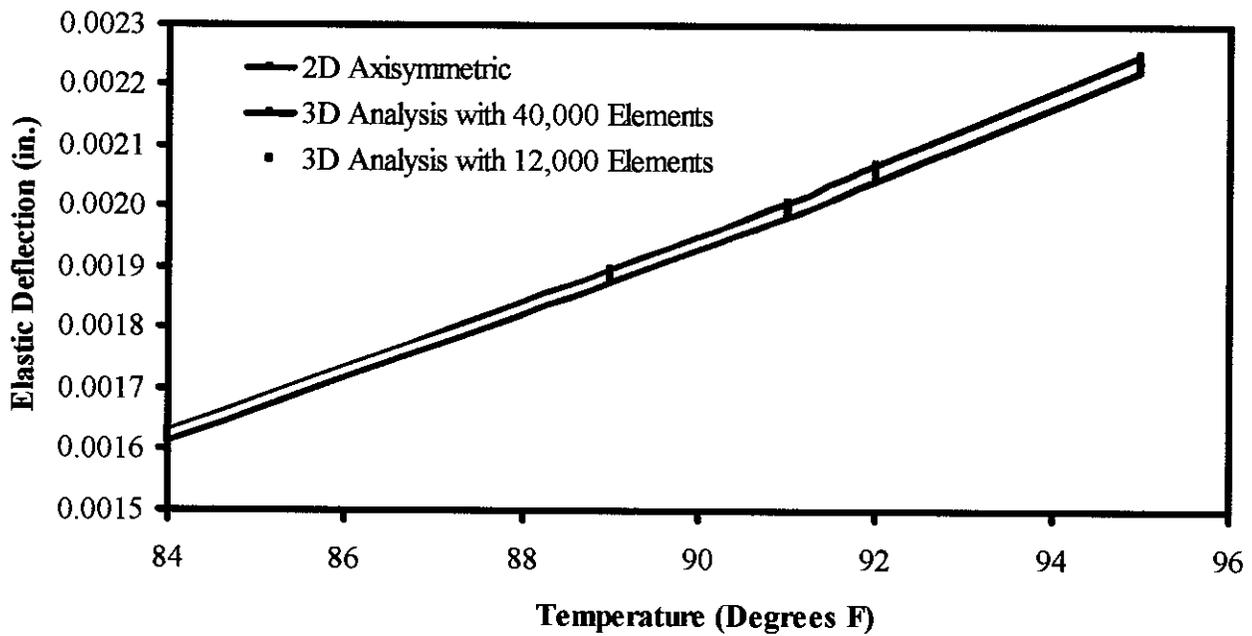**Figure 6.1 ABAQUS 3-D Finite Element Mesh**

Figure 6.2 - Comparison of Results from ABAQUS 3-D, and 2-D Meshes

The rutting model described in Chapter 4 can effortlessly be implemented in the execution of the 3-D meshes as well. This matter further exaggerates the length of time required to execute a realistic problem. To make the models more practical, it may be possible to reduce the number of elements further. As indicated before, reducing the number of elements will introduce some degree of approximation in the results. However, this strategy is not desirable because the main purpose for using the FE models is to minimize any approximation in results. Another alternative is to obtain the primary response of the system from the 3-D FE models and then use these responses with the rutting algorithm described in Chapter 4. We feel that this is a very reasonable compromise between the accuracy and execution time. The process is described below for two cases.

PRIMARY RESPONSE OF 3-D TRIDEM AND TRUNNION AXELS

Three dimensional finite element models were developed to compute the pavement response under trunnion and tridem axles to demonstrate the usefulness of the 3-D model under realistic field and load conditions. The tridem and trunnion axle configurations are shown in Figures 6.3 and 6.4, respectively. The total numbers of tires for the tridem and trunnion, axles are 12 and 16, respectively with the standard widths of 8 ft (2.4 m) and 10 ft (3.0 m)

The analyses were conducted for 1-in. (25-mm), 3-in. (75-mm), and 6-in. (150-mm) thick AC layer. The load was applied at the edge and 2 ft (0.6 m) from the edge to determine the difference in edge versus interior loading. A 10-in. (250-mm) thick base and 14-ft (4.3-m) thick subgrade were used for all analysis. Moduli of 400 ksi (2.8 GPa), 60 ksi (420 MPa) and 10 ksi (70 MPa) were used for the AC, Base and subgrade layers, respectively.

The 1-in. (25-mm) thick AC layer was modeled using six hexahedral elements across its depth. The 3-in. (75-mm) and the 6-in. (150-mm) AC layers were modeled using eight hexahedral elements. For all cases the base was modeled using four layers of hexahedral elements. The top 2 ft (0.6 m) of the subgrade under the pavement was modeled with three layers of hexahedral elements. The rest of the material in the subgrade and the shoulder was modeled using a combination of hexahedral and tetrahedral elements. The same material properties were assumed for the subgrade and shoulder. The use of the tetrahedral elements was necessary to reduce the size of the problem for proper execution in the PC environment. Sufficient mesh refinement exists in the AC layer, the base and at the top of the subgrade, to give accurate results in the regions of interest. To reduce the computing time, only a quarter of the problem area (shown as the shaded rectangular areas in Figures 6.3 and 6.4 were analyzed due to symmetry of the load and geometry for both axle configurations. The FEM mesh for the 6-in. (150-mm) thick AC layer is shown in Figure 6.5. The mesh shown for this picture has about 106,000 elements. All meshes had number of elements ranging from 100,000 to 120,000.

The variation in vertical deflections obtained from the tridem load configuration placed at the edge of the 6-in. (150-mm) thick AC layer is shown in Figure 6.6. Figure 6.7 illustrates the same information but under the trunnion load configuration. Qualitatively, the differences between the distributions of deflections under the two load configurations are appreciable.
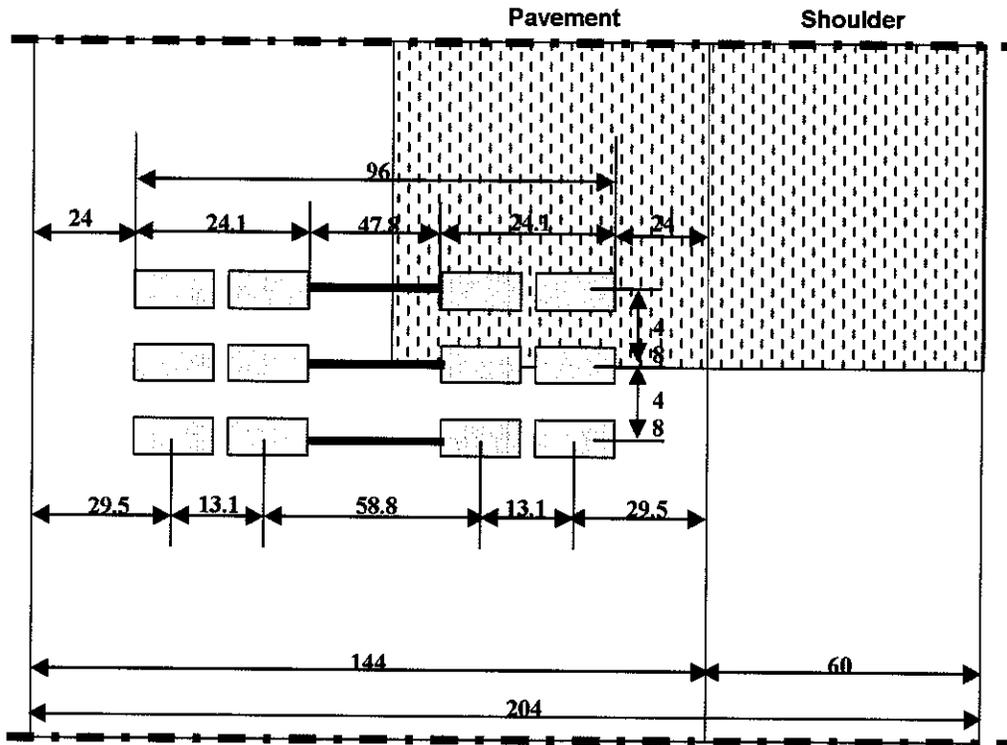
Pavement   Shoulder

96

24   24.1   47.8   24.9   24

4
8

4
8

29.5   13.1   58.8   13.1   29.5

144   60

204

Figure 6.3 - Tridem Load Pattern

Pavement   Shoulder

120

12   51   18   51   12

**Tire Pressure
Area**

60

17.5   13.1   13.8   13.1   29   13.1   13.8   13.1   17.5
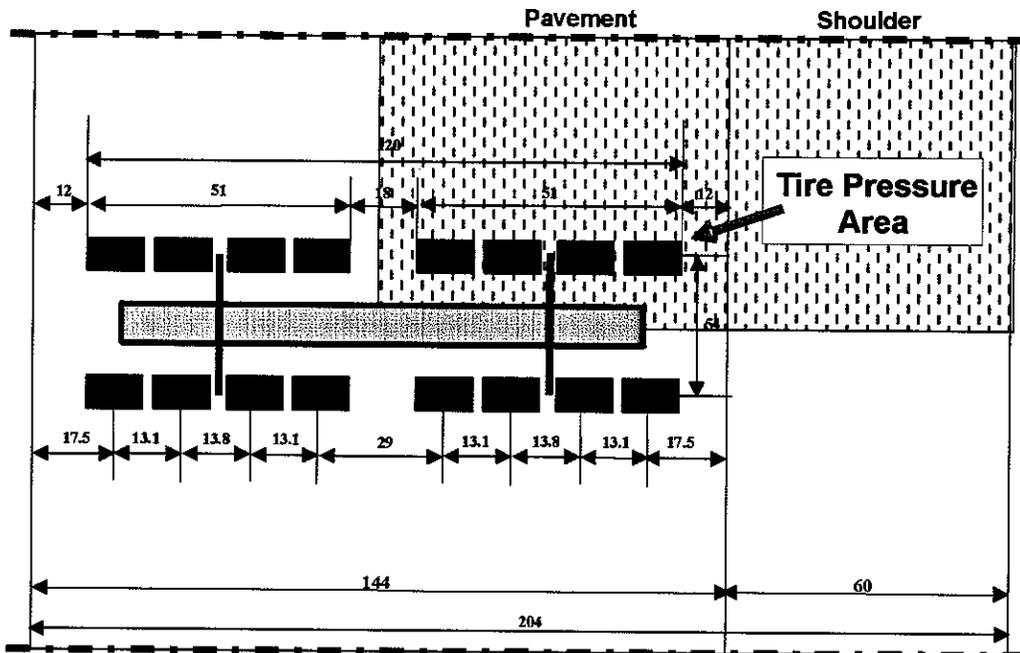
144   60

204

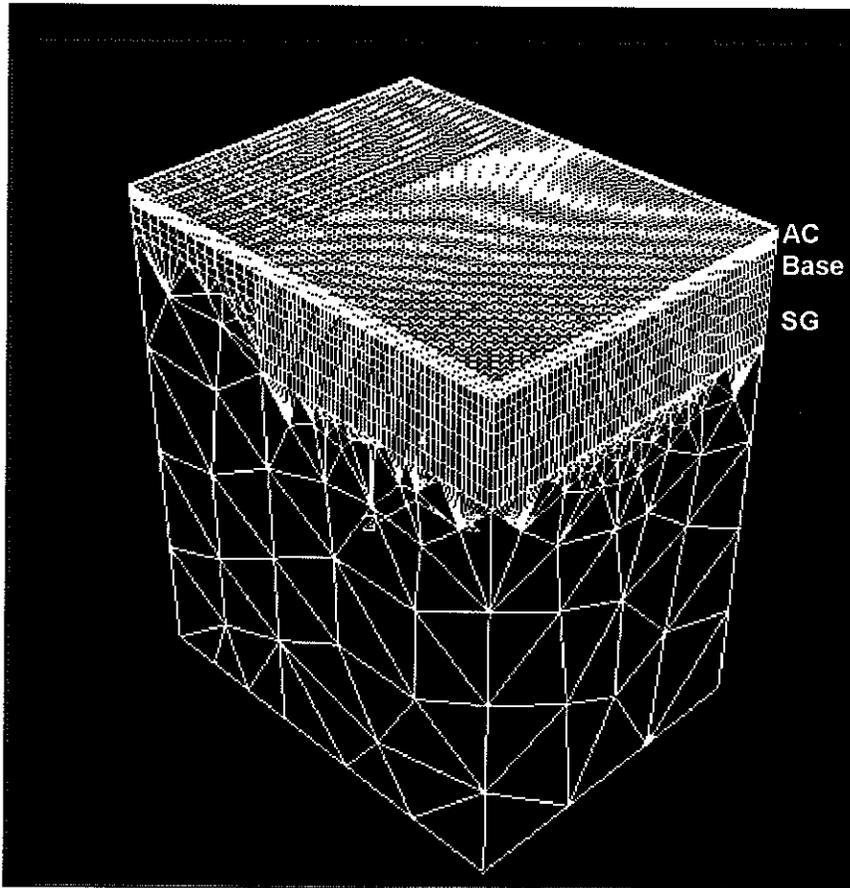**Figure 6.4 - Trunnion Load Pattern**

28

Figure 6.5 - Finite Element mesh for Pavement with 6-in. Thick AC Layer
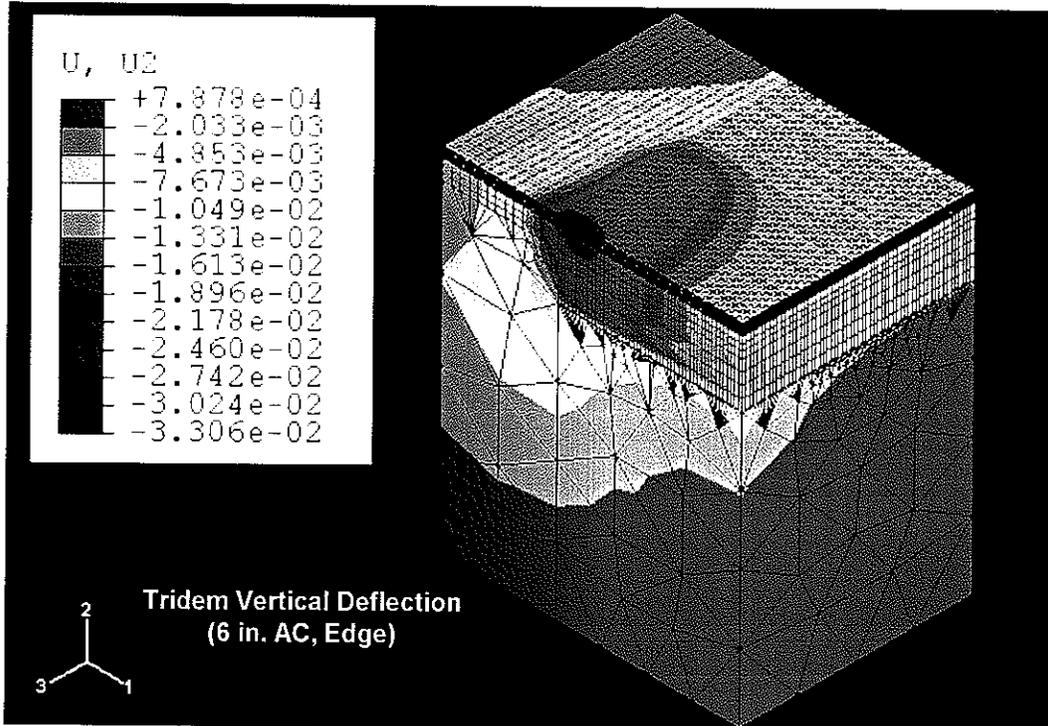
Figure 6.6 – Variation in Vertical Deflection under a Tridem Load Configuration
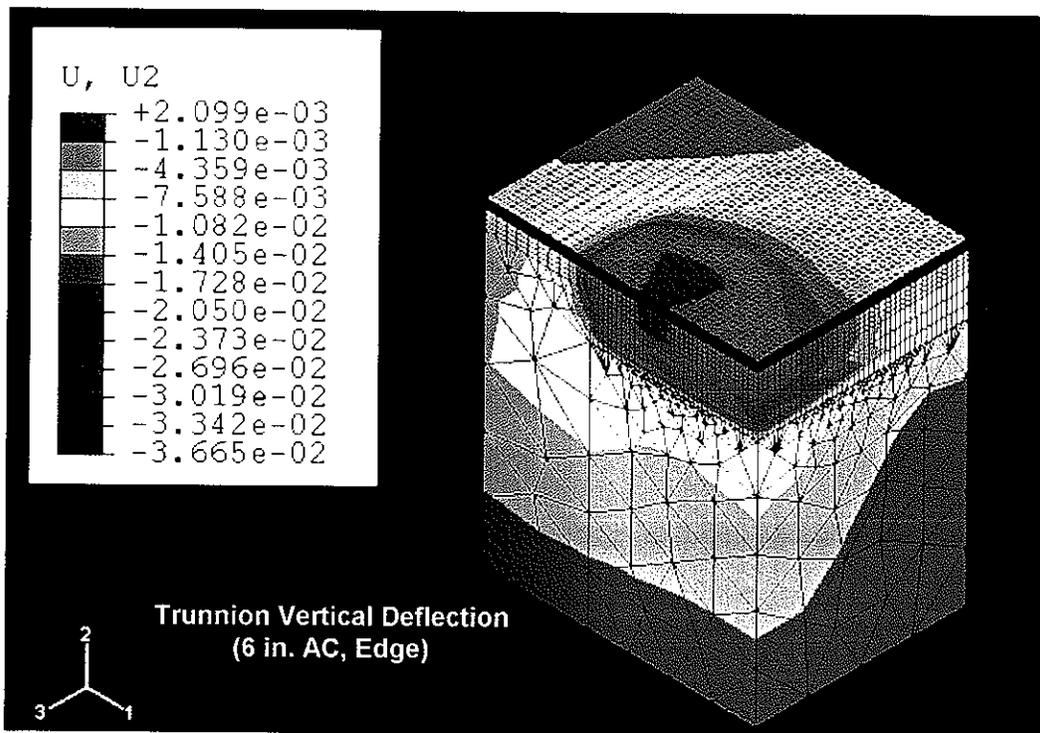

Figure 6.7 – Variation in Vertical Deflection under a Trunion Load Configuration

To quantify the impact of the axle configurations, the results from the analyses on the models indicated above are summarized in Table 6.1. The impact of the axle configuration and the location of the load relative to the shoulder is rather well pronounced in this case. It seems obvious that for a rigorous analysis, pavement discontinuities and load configuration should be rigorously considered.

Table 6.1 Summary of Data for Applied Load at the Shoulder and 2ft. From the Shoulder

AC Thick.	Load Loc.	Tensile Strain (Bottom of AC)		Compessive Strain (Top of SG)		Fatigue Cracking Life		Subgrade Rutting Life	
		Tridem	Trunnion	Tridem	Trunnion	Tridem	Trunnion	Tridem	Trunnion
1 in.	Edge	200	154	720	558	1950	4609	160	502
1 in.	Interior	259	204	653	471	833	1827	248	1072
3 in.	Edge	261	176	621	499.8	812	2970	311	822
3 in.	Interior	232	164	598	384	1203	3747	368	2674
6 in.	Edge	182	135	600	430	2660	7040	363	1611
6 in.	Interior	139	126	452	277	6427	8,921	1288	11539

Strains in microstrain   Lives in 1000 ESALs

In order to reduce the computation time for obtaining the primary response, the mesh can be modified even further. Such a mesh is shown in Figure 6.8. The area close to the load is discretized rather finely; however, for the areas farther away from the area of interest, infinite elements are utilized. The primary responses are mapped to a grid shown in Figure 6.9. The permanent deformation model described in Chapter 4 is then used to compute the rut depth for the number of load applications for each element. The permanent deformations are then summed up to determine a more rigorous variation in permanent deformation for any layer. In that manner, the load-induced nonlinear behavior of the layers can be efficiently determined.

The results from the traditional mesh (shown in Figure 6.1) using the rigorous analysis are compared with those from the new procedure in Figure 6.10. Considering that the computation time for the new procedure is about 1% of the rigorous analysis, and given the uncertainty in material characterization in actual field sites, the results are in very reasonable agreement. The new procedure is a very reasonable compromise between the accuracy and execution time.
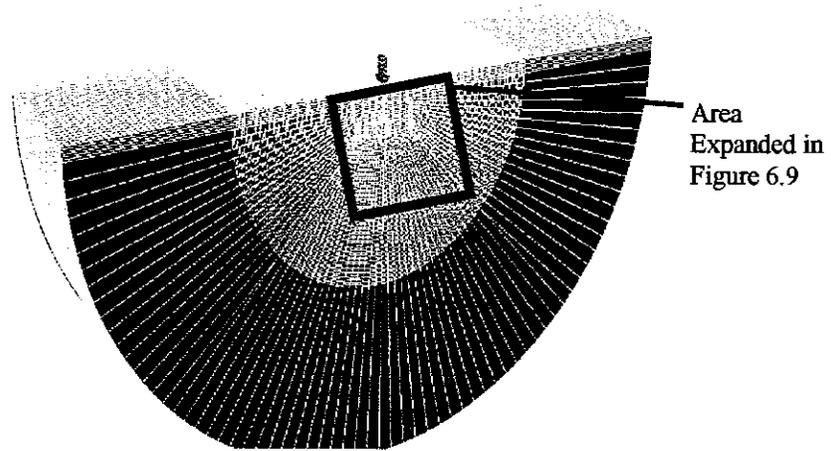
Area
Expanded in
Figure 6.9

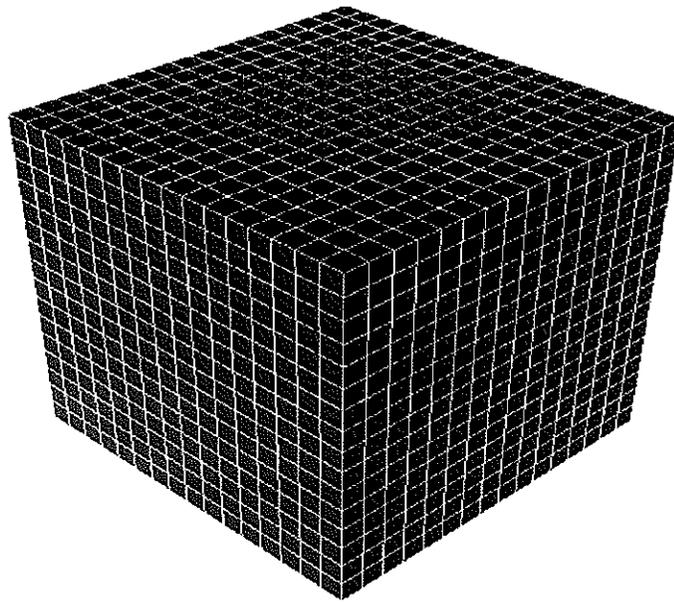**Figure 6.8 – New Efficient Mesh Used to Accelerate FE Executions**

**Figure 6.9 – Refined Mesh Close to Loading area for
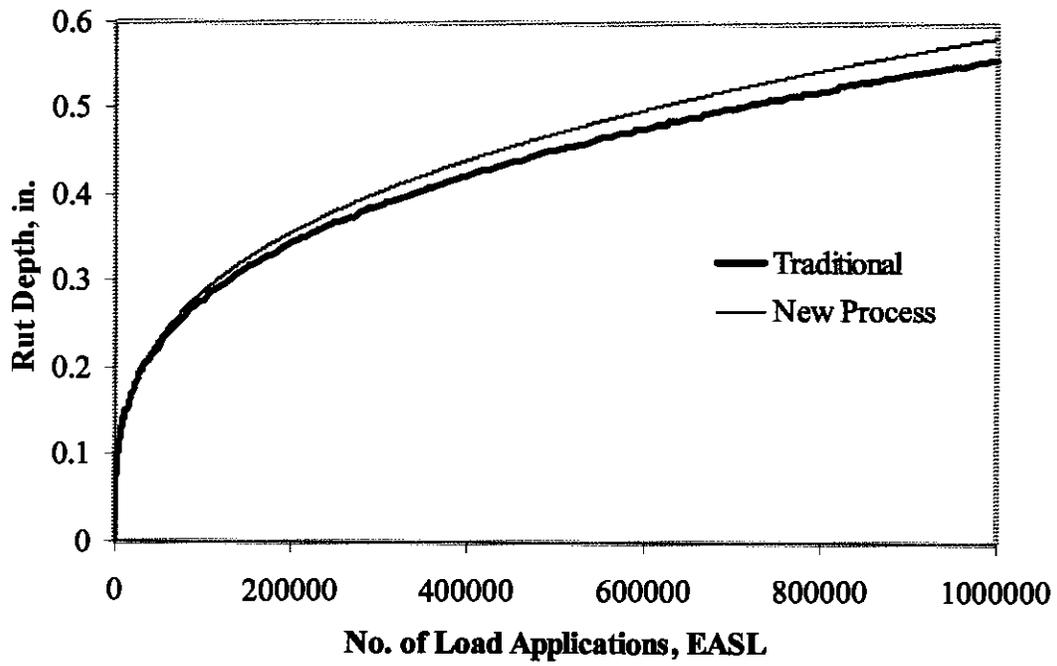Calculating Permanent Deformation**

Figure 6.10 – Variations in permanent Deformation with Load Application from the Rigorous (Traditional) Analysis and Simplified Approach

CHAPTER SEVEN

SUMMARY AND CONCLUSIONS

In this report the use of the two- and three-dimensional finite element analyses to more rigorously estimate the permanent deformation of a pavement section was discussed. The processes of selecting and optimizing the appropriate meshes are discussed. The process for implementing a comprehensive model that considers the nonlinear behaviors of material parameters, load geometry and pavement boundary were described.

In particular the following items were achieved:

- ABAQUS finite element software is selected for this work because of its flexibility in the incorporation of constitutive models.
- Both automatic and manual finite element mesh generation is described and it is showed that automatic mesh provides better results with less number of elements and human efforts.
- The determination of the permanent deformations in ABAQUS is performed in similar fashion as in VESYS.
- The resilient equivalent uniaxial strain is assumed as the resilient strain.
- The finite element, VESYS predictions are reasonably close to the field observations.
- The impact of overload on the rate of rutting was also modeled. For one actual site, a 30% increase in load caused a 50% increase in permanent deformation.
- A rigorous 3-D finite element analysis for determining the permanent deformation of a pavement section is extremely time-consuming
- 3-D Finite element analyses are only necessary when the geometry or load configuration mandates it; otherwise 2-D axisymmetric models are adequate.
- A simplified 3-D approach has been implemented to allow for the determination of permanent deformations at a small fraction of the time necessary for the rigorous analysis.

REFERENCES

- Blab, R.; Harvey, J.T. (2002) "Viscoelastic Rutting Model with Improved Loading Assumptions," Proceedings, Ninth International Conference on Asphalt Pavements, Copenhagen, Denmark.

- Hossain F. and Wu Z. (2002) "Finite Element Simulation of Rutting on Superpave Pavements," Proceedings, Ninth International Conference on Asphalt Pavements, Copenhagen, Denmark.

- Seibi A.C.; Sharma M.G.; Ali G.A. and Kenis, W.J. (2001), "Constitutive Relations for Asphalt Concrete Under High Rates of Loading," Transportation Research Record 1767, Washington, DC.

- Long F., Govindjee S. and Monismith C.L. (2002), "Permanent Deformation of Asphalt Concrete Pavements: Development of a Nonlinear Viscoelastic Model for Mix Design and Analyses," Proceedings, Ninth International Conference on Asphalt Pavements, Copenhagen, Denmark.

- Werkmeister S.; Numrich R. and Frohmut, W. (2002) "Modeling of Granular Layers in Pavement Construction," Proceedings, Ninth International Conference on Asphalt Pavements, Copenhagen, Denmark.

- Zaghloul S. and White T.D. (1994) "Guidelines for Permitting Overloads. Part 1. Effect of Overloaded Vehicles on The Indiana Highway Network. Final Report," Research Report FHWA/IN/JHRP-93/5, Purdue University, West Lafayette, IN

- Zhou F.., and Scullion T. (2002), "Model Calibrations with Local Accelerated Pavement Test Data and Implementation for Focused on Solution to NAFTA Problems", Texas Transportation Institute at Texas A&M University, College Station, Technical report.